



Published in final edited form as:

MAGMA. 2011 June ; 24(3): 121–125. doi:10.1007/s10334-010-0243-6.

Reproducibility of subregional trabecular bone micro-architectural measures derived from 7-Tesla magnetic resonance images

Gregory Chang,

Center for Biomedical Imaging, Department of Radiology, 660 First Avenue, 4th Floor, NYU Langone Medical Center, New York, NY 10016, USA gregory.chang@nyumc.org

Ligong Wang,

Center for Biomedical Imaging, Department of Radiology, 660 First Avenue, 4th Floor, NYU Langone Medical Center, New York, NY 10016, USA

Guoyuan Liang,

Departments of Electrical and Computer Engineering and Radiology, 3414 Seamans Center for the Engineering Arts and Sciences, The University of Iowa, Iowa City, IA 52242, USA

James S. Babb,

Center for Biomedical Imaging, Department of Radiology, 660 First Avenue, 4th Floor, NYU Langone Medical Center, New York, NY 10016, USA

Punam K. Saha, and

Departments of Electrical and Computer Engineering and Radiology, 3414 Seamans Center for the Engineering Arts and Sciences, The University of Iowa, Iowa City, IA 52242, USA

Ravinder R. Regatte

Center for Biomedical Imaging, Department of Radiology, 660 First Avenue, 4th Floor, NYU Langone Medical Center, New York, NY 10016, USA

Abstract

High-resolution magnetic resonance imaging (MRI) of trabecular bone combined with quantitative image analysis represents a powerful technique to gain insight into trabecular bone micro-architectural derangements in osteoporosis and osteoarthritis. The increased signal-to-noise ratio of ultra high-field MR (7 Tesla) permits images to be obtained with higher resolution and/or decreased scan time compared to scanning at 1.5/3T. In this small feasibility study, we show high measurement precision for subregional trabecular bone micro-architectural analysis performed on 7T knee MR images. The results provide further support for the use of trabecular bone measures as biomarkers in clinical studies of bone disorders.

Keywords

Ultra high field; 7 Tesla; MRI; Trabecular bone; Micro-architecture; Knee

Introduction

Over the last decade, high-resolution, magnetic resonance imaging (MRI) has gained importance as a method to detect pathologic alterations in trabecular bone micro-architecture in subjects with osteoporosis [1,2] and osteoarthritis [3,4]. The arrival of high field (HF, 3T) and ultra high-field (UHF, 7T) MR systems can facilitate the high-resolution imaging of trabecular bone. SNR scales approximately linearly with the magnitude of B_0 , and the increased signal-to-noise ratio available at HF/UHF can be converted into increases in spatial resolution or scanning speed. Increased spatial resolution allows for improved visualization of individual trabecular plates and rods that compose the trabecular bone micro-architectural network, and increased scanning speed can reduce patient motion artifact in examinations that can require up to 20 min of imaging time.

The determination of measurement reproducibility for MR-derived structural parameters of trabecular bone is necessary in order to calculate sample sizes for clinical cross-sectional studies or longitudinal studies of disease progression/response to therapy. Previous studies at 1.5/3T have shown reproducibility for MR-derived measures of trabecular bone structure in the distal radius and distal tibia to be less than 7% [5–7]. We hypothesized that similar values could be obtained at 7T. The goal of this feasibility study was to build upon this previous work by determining intra-scan (same day) and inter-scan (different day) reproducibility for trabecular bone micro-architectural analysis performed in a subregional fashion on knee MR images obtained at 7T. Subregional analysis can allow for detection of local (medial vs. lateral) changes in bone structure, as opposed to whole-bone changes [3,4].

Materials and methods

Subjects

This study had institutional review board approval. Three healthy male subjects (35 ± 7.8 years) without history of fracture, musculoskeletal disorder, or bone altering medication use were recruited. Each subject was scanned 3 times; twice within the same day (with re-positioning between scans) and once 7 days later.

MR scanning

The right knee of each subject was scanned on a 7T whole body MR scanner (Siemens Medical Solutions, Erlangen, Germany) using a quadrature knee coil (18 cm diameter, transmit-receive). A high-resolution 3D-fast low angle shot (FLASH) sequence was employed to obtain all images (TR/TE = 20/4.5; flip angle 10 degrees; bandwidth 130 Hz/pixel; one signal acquired; 130 axial images with resolution $0.195 \text{ mm} \times 0.195 \text{ mm} \times 1 \text{ mm}$). Scanning time was ~12 min total.

Image registration

Before image analysis, image registration was applied to the three knee MR data sets in order to ensure that measurements were made in the same location for each subject. The algorithm utilized was based on the mutual information-based rigid-body registration technique [8] (Fig. 1). In brief, the mutual information registration criterion states that the mutual information of the image intensity values of corresponding voxel pairs is maximal if the images are geometrically aligned [8]. After using this registration algorithm to ensure that measurement locations were as similar as possible, image analysis was then performed on the original data sets.

Image processing: segmentation

All images were made anonymous before image processing. A subregional analysis was performed with four different regions of interest (ROIs) around the knee segmented according to the literature [3,4] and as illustrated in Fig. 2. These ROIs were medial and lateral femoral condyle (MFC and LFC), medial and lateral tibial plateau (MT and LT). The medial and lateral tibia plateaus were segmented using a 1×3 grid that fit within the proximal tibia. To adjust the ROI for variation in bone size among the subjects, the dimensions of the grid were standardized based on the epicondylar distance [3,4].

Apparent bone volume fraction (BVF) and marrow volume fraction (MVF) maps

Bone volume fraction (BVF) images were computed using a local marrow intensity computation approach without requiring a global thresholding. In a BVF image, pixel intensity corresponds to the fractional occupancy of bone. Marrow volume fraction (MVF) images were also created by taking the inverse of bone volume fraction images. After subvoxel processing, BVF maps were used directly for fuzzy distance transform. For digital topological analysis, the BVF maps were skeletonized, creating a surface representation consisting of one- and two-dimensional structures (curves and surfaces, respectively).

Fuzzy distance transform (FDT) and quantitative assessment of trabecular bone thickness

At the in vivo spatial resolution of MR images of trabecular bone, the borders of individual trabeculae are indistinct secondary to partial volume effects and noise. Fuzzy distance transform is a method that allows accurate distance measurements in the presence of partial volume effects using gray-scale MR images [9]. FDT at a pixel is computed as the fuzzy distance between the pixel and the background (regions with zero intensity). The thickness of the structure is computed by sampling FDT values along the skeleton of the target structure and then estimating the average.

Digital topological analysis (DTA) and quantitative assessment of trabecular bone and marrow topology

Digital topological analysis is a three-dimensional method that accurately determines the topological class (e.g., surfaces, curves, junctions and edges) of each individual location in a digitized structure that has been applied for quantifying quality of trabecular bone architectural make-up [10]. We computed two specific topological parameters for both trabecular bone and the marrow space: the surface-to-curve ratio and erosion index. The surface-to-curve ratio represents the plate-to-rod ratio, and the erosion index is an inverse marker of network connectivity. In osteoporosis, trabecular surface-curve ratio decreases and trabecular erosion index increases (i.e., decreased trabecular connectivity) [2]. Marrow changes generally reflect the opposite of trabecular changes.

Statistical analysis

For each ROI, mean values for the following parameters were calculated: bone volume fraction; apparent trabecular thickness, surface-curve ratio, and erosion index; marrow surface-curve ratio and erosion index. Mean intra-scan (scans obtained the same day), inter-scan (scans obtained 7 days apart), and inter-subject standard deviations and coefficients of variation (standard deviation divided by the mean) were calculated.

Results

Mean values, standard deviations, and coefficients of variation for micro-architectural parameters are shown in Table 1. The intra-scan and inter-scan coefficients of variation ranged from 0.3 to 5.6% across all regions of interest for all parameters. The inter-subject

coefficients of variation between subjects ranged from 1.2 to 8.3% for trabecular bone morphology and topology and from 2.1 to 11.9% for marrow topology.

Discussion

The goal of this feasibility study was to determine the measurement reproducibility for subregional trabecular bone micro-architectural measures derived from 7T knee MR images. The results demonstrate a low coefficient of variation for measurements obtained on a small number of subjects who were scanned both on the same day and on different days. To our best knowledge, subregional measurement reproducibility for trabecular bone micro-architectural parameters has not been reported previously. Only a handful of publications have described MR imaging of trabecular bone at ultra high-field [11–15] and these studies suggest strong potential for UHF to improve imaging of trabecular bone via increases in spatial resolution or reduced scan times, especially when combined with parallel imaging [12,15]. Overall, the current work provides further support for the use of UHF MR-derived trabecular bone structural parameters in clinical cross-sectional or longitudinal studies of patients with bone disorders.

Knowledge of a technique's measurement precision is important because the standard deviation of the measurement will determine the sample size required to detect a certain difference between groups. Sample size can be given by the formula

$$N = \left(4 \sigma^2 (z_{\text{crit}} + z_{\text{pwr}})^2 \right) / D^2,$$

where N is the total sample size (the sum of the sizes of both comparison groups), σ is the standard deviation, z_{crit} is a value (typically 1.96) that depends on the desired significance criterion (usually set at 0.05), z_{pwr} is a constant (typically 0.842) that depends on the desired statistical power of the study (usually set at 0.80), and D is the minimum expected difference between the groups. The larger the standard deviation of measurement, the larger the total sample size necessary to detect a given difference between groups. As an example, given an intra-scan and inter-scan coefficient of variation of 5.6% (the highest within-subject CV obtained in this study), 20 total subjects would be needed to detect a 5% difference in trabecular parameters in a longitudinal study monitoring disease progression or response to treatment. If the within-subject CV were 10%, a 20-person study would only have enough power to detect a 9% difference over time, and 63 subjects would be needed to detect a 5% difference. Thus, for a given number of study subjects, higher measurement reproducibility allows smaller differences between groups to be detected.

As mentioned previously, a few studies have been described the measurement reproducibility for trabecular bone micro-architectural parameters derived from high-resolution MRI and have shown reproducibility to be less than 7% [5–7]. These studies were performed at 1.5 and 3T, and in only the two more recent studies, [6,7] were subjects scanned on different days. Determining the reproducibility of scanning of subjects on different days is important as this more closely reflects the conditions of a clinical study. For example, in a longitudinal study, the same subject would come back at two-different time points, and in a cross-sectional study, subjects would most likely be scanned on different days.

The spatial resolution of images in this study (0.195 mm in-plane, 1 mm slice thickness) is lower than that described in other 7T MR studies of trabecular bone (0.137–0.195 mm in-plane, 0.41–0.5 mm slice thickness) [11–13,15]. This could affect measurement of trabecular parameters, especially in the slice direction, since the slice thickness is greater

than the thickness of the trabeculae. The mean SNR for trabecular bone in the medial and lateral knee compartments in this study (calculated as the signal intensity (SI) within an ROI drawn on trabecular bone divided by the standard deviation of the SI within an ROI drawn on background) was 9.4 ± 1.3 and 8.7 ± 0.3 , respectively. In the future, the utilization of sequences that provide greater SNR (and spatial resolution) such as steady-state free-precession (SSFP) or fast large-angle spin-echo (FLASE) should allow measurements of trabecular bone structure to be made with even higher precision than reported here [11–13].

There are limitations to this study. One major limitation is the low number of study participants. The main goal of this work as a feasibility study, however, was to show that reproducible subregional measurements can be obtained at 7T, similar to values at 1.5 and 3T. Furthermore, it should be noted that subjects were scanned three times instead of twice, and if anything, a lower number of subjects would likely make high precision harder to achieve. Secondly, we only utilized a 3D-FLASH sequence and did not test other trabecular bone micro-MRI sequences such as SSFP or FLASE, which at 1.5/3T demonstrate high measurement precision [5–7]. Finally, we did not assess measurement reproducibility on any subjects with osteoporosis or bone disorders. It is possible that reproducibility for trabecular parameters may differ in subjects with pathology. In the future, measurement reproducibility for subjects with bone disorders will likely have to be determined as well.

Conclusion

This study demonstrates high reproducibility for subregional trabecular bone micro-architectural measures derived from 7T MR images. Overall, this work provides further support for the use of trabecular bone micro-architectural parameters as biomarkers in clinical cross-sectional or longitudinal studies of disorders affecting bone.

Acknowledgments

The authors would like to acknowledge grant support from the Radiological Society of North America (RR0806) and the United States National Institutes of Health (R01AR056260, R01AR053133).

References

1. Majumdar S. Magnetic resonance imaging of trabecular bone structure. *Top Magn Reson Imaging*. 2002; 13:323–334. [PubMed: 12464745]
2. Wehrli FW. Structural and functional assessment of trabecular and cortical bone by micro magnetic resonance imaging. *J Magn Reson Imaging*. 2007; 25:390–409. [PubMed: 17260403]
3. Blumenkrantz G, Lindsey CT, Dunn TC, et al. A pilot, two-year longitudinal study of the interrelationship between trabecular bone and articular cartilage in the osteoarthritic knee. *Osteoarthritis Cartil*. 2004; 12:997–1005.
4. Lindsey CT, Narasimhan A, Adolfo JM, et al. Magnetic resonance evaluation of the interrelationship between articular cartilage and trabecular bone of the osteoarthritic knee. *Osteoarthritis Cartil*. 2004; 12:86–96.
5. Newitt DC, van Rietbergen B, Majumdar S. Processing and analysis of in vivo high-resolution MR images of trabecular bone for longitudinal studies: reproducibility of structural measures and micro-finite element analysis derived mechanical properties. *Osteoporos Int*. 2002; 13:278–287. [PubMed: 12030542]
6. Gombert BR, Wehrli FW, Vasilic B, et al. Reproducibility and error sources of micro-MRI-based trabecular bone structural parameters of the distal radius and tibia. *Bone*. 2004; 35:266–276. [PubMed: 15207767]
7. Wald MJ, Magland JF, Rajapakse CS, Wehrli FW. Structural and mechanical parameters of trabecular bone estimated from in vivo high-resolution magnetic resonance images at 3 Tesla field strength. *J Magn Reson Imaging*. 2010; 31:1157–1168. [PubMed: 20432352]

8. Maes F, Collignon A, Vandermeulen D, Marchal G, Suetens P. Multimodality image registration by maximization of mutual information. *IEEE Trans Med Imaging*. 1997; 16(2):187–198. [PubMed: 9101328]
9. Saha PK, Wehrli FW. Measurement of trabecular bone thickness in the limited resolution regime of in vivo MRI by fuzzy distance transform. *IEEE Trans Med Imaging*. 2004; 23:53–62. [PubMed: 14719687]
10. Saha PK, Gomberg BR, Wehrli FW. Three-dimensional digital topological characterization of cancellous bone architecture. *Int J Imaging Syst Technol* 2000. 2000; 11:81–90.
11. Krug R, Carballido-Gamio J, Banerjee S, et al. In vivo bone and cartilage MRI using full-balanced steady-state free-precession at 7 Tesla. *Magn Reson Med*. 2007; 58:1294–1298. [PubMed: 17957777]
12. Banerjee S, Krug R, Carballido-Gamio, et al. Rapid in vivo musculoskeletal MR with parallel imaging at 7T. *Magn Reson Med*. 2008; 29:655–660. [PubMed: 18224700]
13. Magland J, Rajapakse CS, Wright AC, Acciavatti R, Wehrli FW. 3D fast spin echo with out-of-slab cancellation: a technique for high resolution structural imaging of trabecular bone at 7 Tesla. *Magn Reson Med*. 2010; 63:719–727. [PubMed: 20187181]
14. Chang G, Pakin SK, Schweitzer ME, Saha PK, Regatte RR. Adaptations in trabecular bone microarchitecture in Olympic athletes determined by 7T MRI. *J Magn Reson Imaging*. 2008; 27:1089–1095. [PubMed: 18425824]
15. Chang G, Friedrich KM, Wang L, et al. MRI of the wrist at 7 Tesla using an eight-channel array coil combined with parallel imaging: preliminary results. *J Magn Reson Imaging*. 2010; 31:740–746. [PubMed: 20187221]

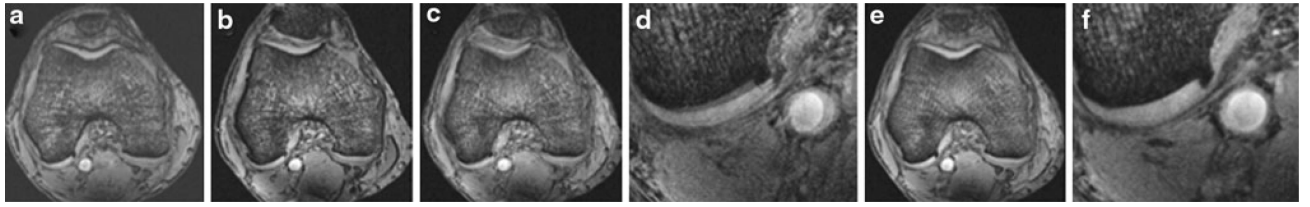


Fig. 1.

Illustration of retrospective MR image registration of a knee. All methods were applied in three dimensions. **a, b** Two 3D-MR data sets of a knee were acquired 7 days apart. **c, d** The image obtained by simply adding the two original MR image data sets prior to applying any image registration method. **d** Is a zoomed-in portion of (**c**). The double edging effect is visually evident indicating spatial misalignment of matching anatomic structures in original MR images. **e, f** Same as (**c, d**) but after applying image registration on the two MR data sets. Double edging is significantly reduced after applying image registration in (**e, f**), which depicts spatial alignment of matching anatomic structures in two registered images

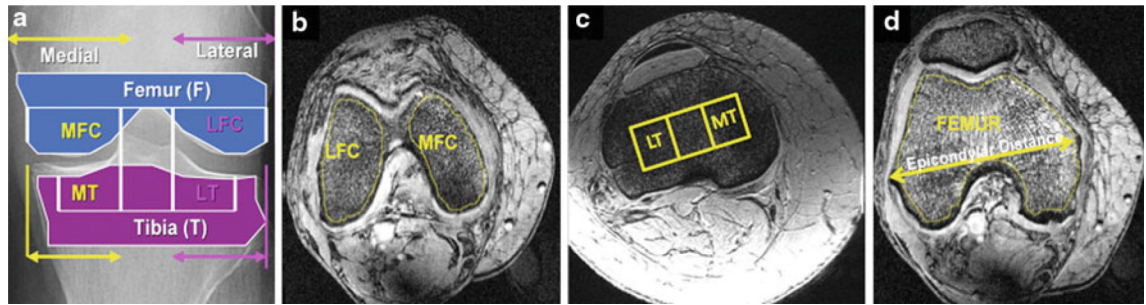


Fig. 2.

Four different regions of interest (a) within the medial and lateral femoral condyles (b) and medial and lateral tibial plateaus (c) were segmented for trabecular bone and marrow analysis. The medial and lateral tibial plateaus were segmented using a 1×3 grid that fit within the proximal tibia. To adjust the ROI for variation in bone size among the subjects, the dimensions of the grid were standardized based on the epicondylar distance (d). *MFC* medial femoral condyle, *LFC* lateral femoral condyle, *MT* medial tibia, *LT* lateral tibia

Table 1

Mean values for subregional trabecular and marrow micro-architectural parameters derived from 7 Tesla knee MR images

MRI parameter and location	Mean	SD	CV (%)			
			Intra-scan	Inter-scan	Intra-subject	Inter-subject
<i>Trabecular morphology</i>						
BVF						
LFC	0.289	0.001	0.004	0.005	0.005	2.0
LT	0.296	0.005	0.001	0.010	0.010	3.7
MFC	0.272	0.007	0.005	0.010	0.010	4.3
MT	0.294	0.003	0.006	0.009	0.009	4.2
Th.Th						
LFC	0.233	0.006	0.005	0.005	0.005	2.8
LT	0.222	0.007	0.002	0.001	0.001	1.9
MFC	0.244	0.004	0.003	0.001	0.001	1.4
MT	0.229	0.009	0.004	0.013	0.013	6.4
<i>Trabecular topology</i>						
SCR						
LFC	7.429	0.102	0.092	0.616	0.616	8.3
LT	6.839	0.163	0.097	0.161	0.161	2.4
MFC	7.542	0.117	0.136	0.307	0.307	4.1
MT	7.353	0.097	0.159	0.265	0.265	3.6
EI						
LFC	0.852	0.008	0.006	0.009	0.009	1.2
LT	0.933	0.017	0.029	0.052	0.052	5.6
MFC	0.806	0.009	0.013	0.027	0.027	3.4
MT	0.887	0.008	0.014	0.013	0.013	1.5
<i>Marrow topology</i>						
SCR						
LFC	25.021	0.691	0.644	2.470	2.470	9.9
LT	19.643	0.946	1.090	2.320	2.320	11.8
MFC	20.650	1.103	0.671	1.173	1.173	5.7
MT	19.768	0.639	0.896	1.403	1.403	7.1

MRI parameter and location	Mean	SD	CV (%)							
			Intra-scan	Inter-scan	Inter-subject	Intra-scan	Inter-scan	Inter-subject		
EI										
LFC	0.305	0.004	0.006	0.006	0.006	1.5	2.0	2.1		
LT	0.336	0.007	0.006	0.039	0.039	2.2	1.8	11.9		
MFC	0.304	0.011	0.009	0.007	0.007	3.6	3.3	2.6		
MT	0.344	0.005	0.005	0.019	0.019	1.5	1.7	5.7		

Mean intra-scan (same day scans with re-positioning in between), inter-scan (scans 7 days apart), and inter-subject standard deviations (SD) and coefficients of variation (CV) are shown. (LFC)lateral femoral condyle, LT lateral tibia, MFC medial femoral condyle, MT medial tibia, BVF bone volume fraction, Tb.Th apparent trabecular thickness, SCR surface-curve ratio, EI erosion index)